

Experimental Study of the Cooling Characteristics of Polymer Filaments in FDM and Impact on the Mesostructures and Properties of Prototypes.

Q. Sun, G.M. Rizvi, C.T. Bellehumeur^{1*} and P.Gu²

¹Department of Chemical and Petroleum Engineering
²Department of Mechanical and Manufacturing Engineering
University of Calgary, Calgary, Alberta, T2N 1N4 Canada

Reviewed, accepted August 19, 2003

Abstract

The bonding quality among polymer filaments in the fused deposition modeling (FDM) process determines the integrity and mechanical properties of the resultant prototypes. This research investigates the bond formation among extruded acrylonitrile butadiene styrene (ABS) filaments in the FDM process. Experimental measurements of the temperature profiles were carried out for different specimens and their effects on mesostructures and mechanical properties were observed. Models describing the formation of bonds among polymer filaments during the FDM process are discussed. Predictions of the degree of bonding achieved during the filament deposition process were made based on thermal analysis of extruded polymer filaments. The bond quality was assessed based on the growth of the neck formed between adjacent filaments and their failure under flexural loading. Further experimental work is underway to assess the validity of the proposed models.

1. Introduction

Rapid prototyping (RP) is one of the fastest growing manufacturing technologies for fabrication of cost effective models, prototypes and one of a kind parts. It is being applied in a very large number of fields, such as aerospace, automotives, architecture, and medicine. RP technologies provide the ability to create almost completely finished products from CAD files. Moreover, it has been shown that some RP techniques have the potential to fabricate parts with locally controlled properties (porosity, density and mechanical properties) [1,2]. The FDM machine is basically a computer numerically controlled (CNC) gantry machine, carrying double miniature extruder head nozzles. In the FDM process, parts are fabricated by extruding a semi-molten filament through a heated nozzle in a prescribed pattern onto a platform. As the material is deposited, it cools, solidifies and bonds with the surrounding material. The fabrication of parts with locally controlled porous structure and mechanical properties can be achieved by varying the deposition strategy, deposition orientation and other process conditions. However, for directly producing functional parts, fundamental understanding of mechanical properties of FDM parts with respect to fabrication process parameters is essential.

* Corresponding Author: C.T. Bellehumeur, cbellehu@ucalgary.ca, tel.: (403) 220-8804, fax: (403) 282-3945

FDM prototypes are composites of partially bonded filaments and voids. The bonding quality among filaments in FDM parts is an important factor in determining the integrity and mechanical properties of resultant prototypes. The formation of bonds in FDM process is driven by the thermal energy of semi-molten material. The quality of bonds formed between individual filaments depends on the growth of the neck formed between adjacent filaments and on the molecular diffusion and randomization at the interface. The bond formation process can be viewed as a sintering process for which the wetting phenomenon is of importance. It can also be modeled following approaches similar to those used to describe polymer welding, where the issue of molecular diffusion dominates.

Studies in FDM have primarily been directed towards the development of new materials or techniques for material deposition [3-5]. The mechanical properties of filaments and FDM parts were also investigated by a number of researchers [6-8]. However, considerable research efforts are still needed to fully understand the mechanical properties and their relations to the fabrication processes. In particular there is a lack of literature on experimental determination of the thermal profiles of the parts built using FDM. This data is especially important, as it is indicative of the bond formation between adjacent filaments. This paper provides the results of experimental determination of the thermal profiles of some simple shapes produced using the FDM process and their effects on the bond formation in terms of neck growth between adjacent filaments and the intermolecular diffusion at the interface and their evaluation in regards to the mechanical properties of the parts.

2. Experimental Work

The FDM 2000 from Stratasys Inc was used in this study. A commercial acrylonitril butadiene styrene (ABS P400) was used. The material was heated to 270°C and extruded through a nozzle onto a platform. The envelope temperature was set to 70°C. All parts were built using tip 12 with zero air gap. In addition, parts produced in this study consisted of unidirectional specimens to enhance the effects of the parameters being studied. The parts produced for mesostructure characterization and for mechanical testing were built with the normal five layers of support material. As the support material may have different characteristics, the parts generated for the measurements of the filament's temperature profile were built without the support layers.

The temperature profiles of extruded filaments were monitored using 0.003" K type thermocouples. The thermocouples were imbedded in the foam of the base plate of the FDM machine. The measurements were recorded and analysed through a high-frequency analog-digital converter (1000 readings per second), amplifier, data acquisition card 6024E and software Labview 6.0 on a PC.

The samples collected from the parts were sectioned using a Leica RM2165 microtome. The samples' cross-sections were viewed under optical microscopy. Pictures of these cross-sections were taken with a CCD camera mounted on an Olympus BX60 microscope and features were analyzed using the image analysis software Image-Pro[®].

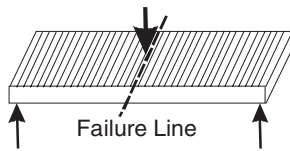


Figure 1: Flexural strength test sample

The flexural strength testing of the specimens was carried out on the ATM testing machine (Model TTS Series). The tests conformed to ASTM standard D 1184-98 for flexural strength of laminated sheets bonded with glue. The specimens were constructed so that the failure occurs in the bonds between adjacent filaments as shown in Figure 1. One deviation from the standard was that failure occurred between filament bonds in the same layer instead of the bonds between adjacent layers. The test also differed from the standard in that 12 layers of laminates were used instead of the stipulated eight layers, so that parts with reasonable dimensions could be tested.

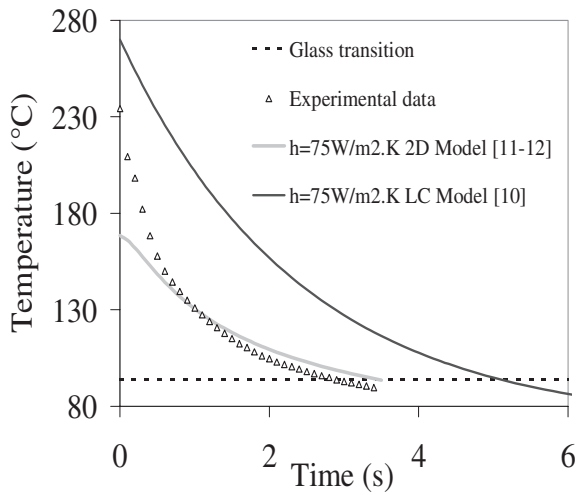
3. Thermal Processes in FDM

The bonding between individual roads of the same layer and of neighboring layers of FDM parts is driven by the thermal energy of the semi-molten material that is extruded from the FDM head. The temperature history of interfaces plays an important role in determining the bonding quality. When the filament is deposited and is in contact with surrounding material, the interface's temperature is well above the material's glass transition (T_g). This condition favors molecular diffusion at the interface and the development of adhesive bonds.

Several heat transfer models describing the FDM process have been proposed in the literature. Yardimci [9] developed a family of numerical models for the fused deposition ceramic (FDC) processes. A similar analysis method is applicable to the FDM process that uses thermoplastic polymer as a raw material. Rodríguez-Matas [10] presented a two-dimensional heat transfer model in which the filament is laid on a stack of other filaments. The model assumes constant heat convection coefficient and perfect contact among stacked filaments. The results of the analysis show that the interface temperature rises above the glass transition temperature (T_g) immediately upon extrusion of the filament and stays above for a short period of time. In Rodríguez's analysis, the variations in the temperature across the filament thickness are taken into consideration, which allows for consideration of the boundary conditions at the interface. The model, however, neglects all contact resistances between the filaments. Based on this 2D model, the conduction heat transfer with the foundation is dominant over the convection heat transfer with the environment. Li and co-workers [11-12] used the lumped-capacity analysis for modeling the cooling process of the extruded filament, because the diameter of the extruded filament is fairly small and a uniform temperature distribution throughout the filament cross-section can be assumed.

3.1. Temperature Profile of a Single Filament

Experimental measurements performed on a single filament deposited on the base plate foam platform were used to assess the validity of the two models described above (Figure 2). The material properties were selected based on the work presented by Li et al. [12]. The measured data is in general agreement with these models, lying somewhere in between the two predicted values. It is interesting to note that at the higher temperatures prevailing in the initial



stage, the measured temperature profile exhibits more similarity to the lumped capacity model predictions, while at lower temperatures the measured data tends to follow the 2D model predictions [10]. The filament reached T_g in about three seconds, which is not very different from the predictions of both models.

Figure 2: Single filament cooling profile where h denotes the convective heat transfer coefficient.

3.2. Multi Layered Specimen: Temperature Profiles and Mechanical Tests

Two sets of specimens were constructed to carry out mechanical tests in order to assess the bond strength between the filaments. The dimensions of the test specimens were 3.1 mm x 19.1 mm x 31 mm, and all the filaments were oriented perpendicular to the longitudinal axis of the parts for the tests so that failure would occur in the bonds between the adjacent filaments of the lower layer as shown in Figure 1. In the first set, the specimens were built individually, whereas for the second set, three specimens were cut from one longer piece (Figure 3a). The temperature profiles at the base of each representative specimen were also recorded and are shown in Figure 3b.

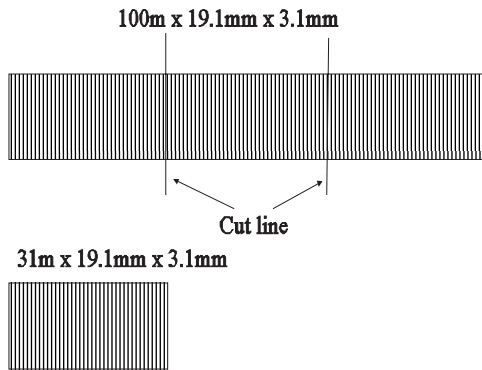


Figure 3a: Different specimens for flexural strength tests

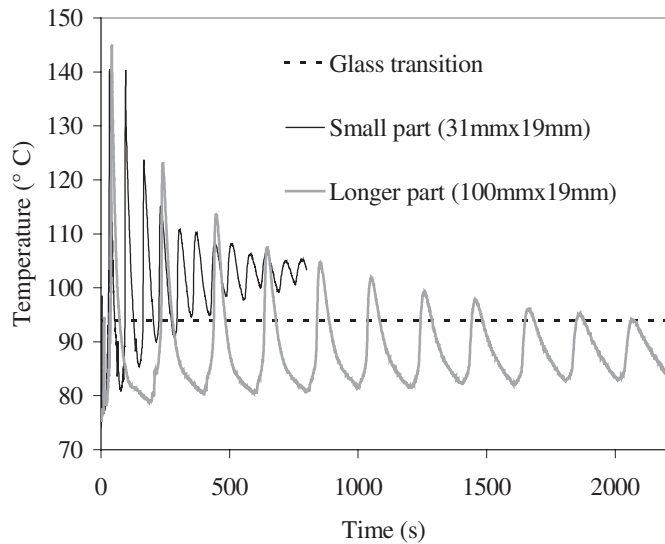


Figure 3b: Comparison of the temperature profiles for different specimens

One must note that the highest temperatures recorded in these profiles were lower than that measured for a single filament. This was due to the fact that a larger set of data (1000) was averaged to get one record per second, compared to 100 records per second for the previous case. Therefore, the higher values were averaged with lower values to give smaller peaks. Secondly, the models discussed in the previous section are only valid for single roads and cannot be applied to the situation represented in this case, where conduction is the dominant mode of heat transfer from the adjacent and upper layer filaments. It can be seen that for the specimens built individually (first set) the temperature at the base of the part remains above the glass transition temperature (T_g) after the 4th layer is built and continues to be high until the parts are completed. For the second set of specimens, the temperature reaches a level above T_g for only a short duration during the deposition of each layer of filaments. Therefore, it is to be expected that the individually made specimens will be stronger than the specimens cut from longer pieces. This expectation is indeed borne out by the mechanical testing and the results are shown in Table 1. The flexural strength of the individually made specimens was 2810 kPa, whereas, it was 2277 for the specimens cut from the larger part. The higher temperature profile, which gave rise to higher flexural strength, was the result of the shorter traverse of the FDM head for making one layer of the individually built specimen compared to the three times larger traverse to build the longer part from which three specimens were cut. This resulted in better bonding between the adjacent filaments and consequently the individually built parts exhibited higher failure loads.

The test data exhibited a much larger standard deviation in the results of the specimens cut from the longer parts (Table 1). This deviation could be the result of two possible factors. The first was that a number of larger parts exhibited miniature fault lines between adjacent filaments. One possible cause of these faults could be the wear in the mechanical system of the FDM machine. The obviously faulty samples were discarded on visual inspection, but if the fault was in the inner layers, or too small, it would escape visual inspection. Another factor was that the temperature profile was observed to change with variations in the location of the parts built. This would cause variation in exposure temperature/time of the parts being built. Further experimentation is required before drawing any definite conclusions.

Part type	Cut from longer piece	Individually built
Flexural strength (kPa)	2277.0	2810.0
Standard deviation (kPa)	105.9	87.2
Total samples used	8	4

Table 1: Comparison of the flexural strength for individual parts of different size

Layer undergoing failure	Bottom	Top
Flexural strength (kPa)	2277.2	2153.6
Standard deviation (kPa)	105.9	65.9
Total samples used	8	5

Table 2: Comparison of the flexural strength for failure in the top vs. bottom layers of the specimens cut from the longer part

The temperature profile of the longer part shown in Figure 3b also suggests that the top layers of the specimen are exposed to shorter durations of temperature above T_g compared to the lower layers. This would indicate that the lower layers of the specimen should have higher bond strengths than the upper layers. To verify this, a number of samples were prepared and tested so

that the failure would occur either in the top or in the bottom layer of the specimens, and the results are shown in Table 2. Indeed, the bottom layers did exhibit higher bonding strength between the adjacent filaments. The flexural strength of the specimen when the fracture was caused to occur in the bottom layer was 2277 kPa against a value of 2153 kPa when the fracture was caused to occur in the top layer. Again the standard deviation was quite large, since the specimens were cut from the longer parts as already discussed above.

3.3. Effects of Prolonged Exposure to Higher Temperatures on the Mesostructure

It was generally observed that the temperature profile of the bottom layers of the parts remains at temperatures higher than T_g for a longer period of time compared to the upper layers. Thus, different neck growth between adjacent filaments can be expected in the top and bottom regions. However, this phenomenon was not readily observable in a twelve-layer specimen. Consequently, thirty-layer specimens were prepared. Figure 4 shows a magnified picture and the temperature profile for these specimens. As can be seen, after the first few layers, the temperature was above T_g until the completion of the part. The voids in the lower region are clearly smaller than in the upper region indicating larger neck growth in the bottom of the part. The dimensionless neck growth in the top few layers is 0.187 compared to 0.310 in the bottom layers. One possible explanation for the larger neck growth could be the longer diffusion time as discussed in the later sections dealing with modeling. Other explanations could be the effect of gravity or the effect of continued downward pressure from the FDM head while the part is being built.

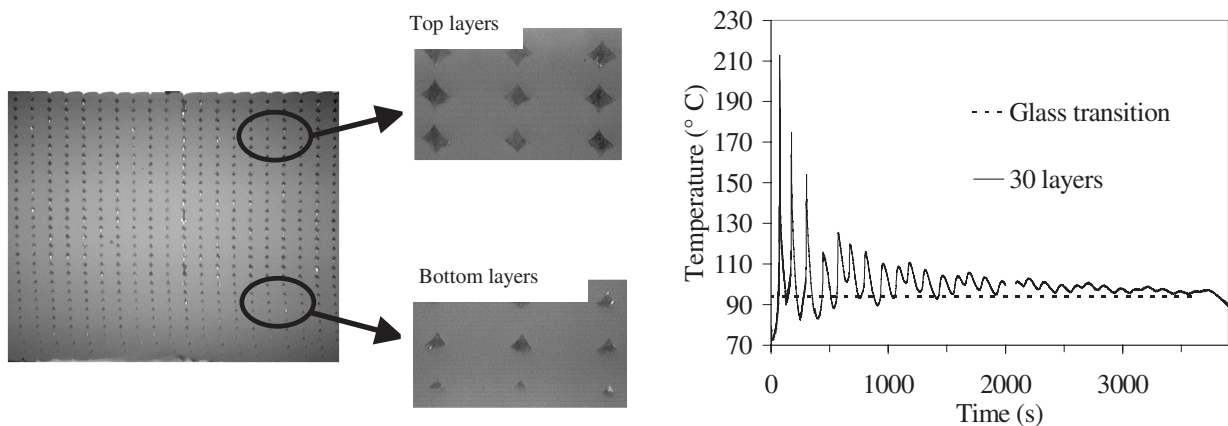


Figure 4: Mesostructure and temperature profile of a 1.5'' x 1.5'' x 30-layer part

3.4. Effects of Filament's Deposition Strategy on Temperature Profiles and Mesostructures

The impact of the deposition strategy on the parts' characteristics was examined in this work. Figure 5 shows the temperature profile at the base of a part with dimensions 200 mm x 12 mm x 2.8 mm in which the filaments were deposited in the longitudinal direction. After the second layer is formed, the temperature at the base remains above T_g for the duration of the build time. Figure 6 shows the temperature profile at the base of a part with dimensions 130 mm x 28 mm x 2.8 mm in which the filaments were deposited in the lateral direction. Due to the short path

length, the temperature reaches much higher values as the FDM head approaches the thermocouple, but later drops below the T_g limit as the head recedes. In this case the part is exposed to higher temperature for a longer time. Table 3 summarizes the results obtained for the dimensionless neck formed between adjacent filaments. The lateral specimen exhibits a higher dimensionless neck growth, and consequently has a lower void fraction due to longer exposure to higher temperatures.

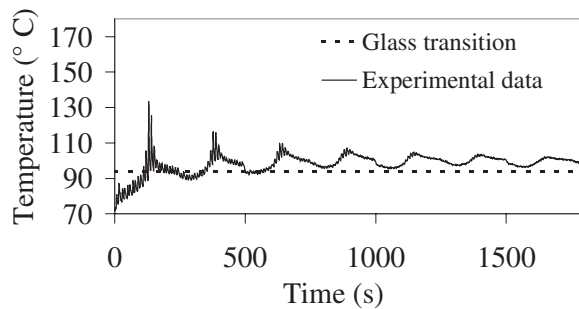


Figure 5: Temperature profile for a longitudinally built part

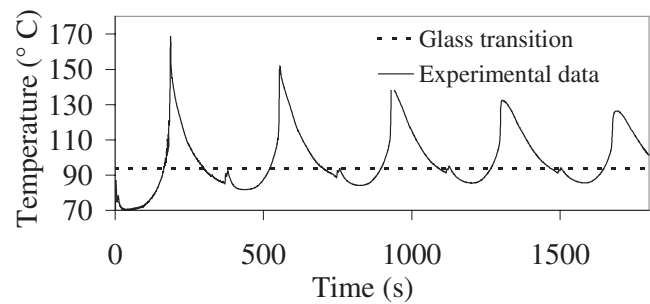


Figure 6: Temperature profile for a laterally built part

	Longitudinal parts	Lateral parts	Top layers (30-layer part)	Bottom layers (30-layer part)	Sintering model prediction
Dimensionless Neck growth	0.191	0.233	0.187	0.310	0.152
Void fraction (%)	0.091	0.081	--	--	--

Table 3 Dimensionless neck growth and void fraction for various parts

4. Prediction of Bond Formation

The formation of bonds between polymer filaments in the FDM process can be described as shown in Figure 7. The cross-sections of filaments are idealized as circles in the figure. The first step of the process is the establishment of interfacial molecular contact by wetting. The molecules then undergo motions toward preferred configurations to achieve the adsorptive equilibrium [9]. Molecules diffuse across the interface, forming an interfacial zone, and/or react to form primary chemical bonds across the interface. The randomization can be reached only after extensive inter-diffusion of chain segments under critical conditions. These processes can be interpreted either in terms of sintering of adjacent particles or inter-diffusion of molecules at the contact interface, both of which occur at elevated temperatures. Predictive models, for both sintering and diffusion, which utilize the measured temperature profiles, are discussed in the following sections.

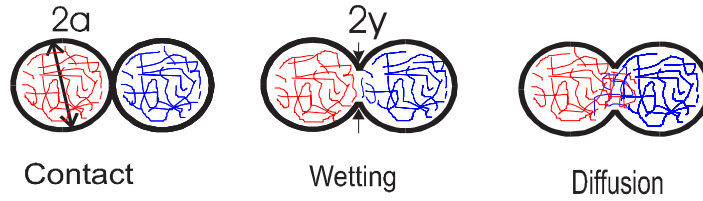


Figure 7: Schematic of bond formation between two filaments

4.1. Sintering Model

Analytical models describing the sintering rate that occur, due to Newtonian and viscoelastic flows, in various polymers have been proposed and assessed by Hornsby and Maxwell [13], Mazur and Plazek [14], and Bellehumeur et al. [15-16]. In this work, the model proposed by Pokluda and co-workers [17] has been used.

$$\frac{d\theta}{dt} = \frac{\Gamma}{a_o\mu} \frac{2^{-5/3} \cos \theta \sin \theta (2 - \cos \theta)^{1/3}}{(1 - \cos \theta)(1 + \cos \theta)^{1/3}} \quad (1)$$

with $\theta = \sin^{-1} y/a$. The model is valid for the coalescence of two particles and predicts the neck growth between the particles as a non-linear function of time t , material viscosity μ , initial particle radius a_o , and surface tension Γ . Details on the mathematical development and assessment of the model have been discussed elsewhere [11-12].

The sintering model is used to determine the neck growth formation between the sintering particles, thus providing information about the degree of wetting achieved at the filaments' interface, which is an indication of the neck growth. Previous work [1] has shown that the neck growth becomes negligible at temperatures below 200°C for ABS P400. This temperature is to be referred to as the critical sintering temperature for ABS P400. Quantitative predictions about the degree of bonding achieved during the filament deposition process were made based on the lumped-capacity heat transfer and Newtonian sintering models. The selection of model parameters was based on criteria presented in reference [12]. These results were found to be only in general agreement with the experimental observations (Table 3). Quantitatively, the difference might be due to simplifying the cross-section shape of the filament (circle versus ellipse), neglecting gravity force in the sintering model and neglecting elastic deformation that may occur at temperatures below the critical sintering temperature.

4.2 Diffusion Model

The theory of intermolecular diffusion across the interface under isothermal conditions is well established in literature. The isothermal models work quite well for quasi-isothermal processes such as autoclaving. However, for on-line consolidation type processes such as FDM, where thermal transients are present at multiple time scales, a non-isothermal model is needed. A

model put forwarded by Fang [18] for the healing process under non-isothermal conditions was used to predict bond strength. The model considers a temperature dependent welding time and describes the bond strength as a function of the temperature history. The non-isothermal degree of healing evolution with time is developed starting from a fundamental formulation of the reptation of polymer chains and is given by the following expression:

$$D_h(t) = \frac{\sigma}{\sigma_\infty} = \left[\int \frac{1}{t_w(T)} dt \right]^{1/4} \quad (2)$$

where $t_w(T)$ is the temperature dependent welding time, σ_∞ is the strength of the fully healed interface, and σ is the stress for the FDM part. For a given temperature history, and a given temperature dependence of the welding time, the degree of healing can be evaluated using equation 2. The respective temperature profiles in conjunction with the extruded ABS P400 welding time, as determined by Rodríguez [8], were used to quantitatively predict the bond strength of the parts produced for mechanical testing. The welding time used is only valid in a very narrow temperature range and needs to be re-examined at higher temperatures in future work.

$$t_w = C \exp(Q_d / RT) \quad (3)$$

where $Q_d = 388.7$ kJ/mol and $C = 1.080 \times 10^{-47}$ s.

The model described by equation 2, was implemented numerically to predict the degree of healing as a function of time. The numerical integration was carried out until the degree of healing reached a value of unity, or until the specified time was completed, whichever occurred first. Furthermore, for amorphous materials the healing mechanism is active only as long as the material temperature is above its glass transition point, hence only that time when the temperature was above the glass transition point was taken into consideration.

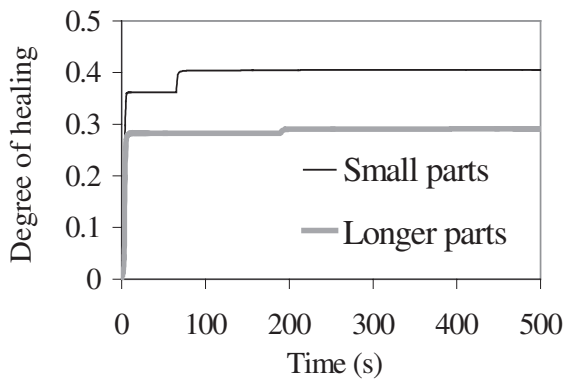


Figure 8: Degree of healing of FDM parts with different temperature histories

The modeling results are shown in Figure 8. From Figure 3b it can be seen that the individually produced parts stay above glass transition temperature longer and consequently have a higher degree of healing with the resultant higher bond strength. Figure 8 shows a drop of 28% in the degree of healing for the longer part from which the three specimens were cut. However, the drop in the load bearing capacity of these specimens was only about 10%. The difference can be attributed to the available welding time data, which covers only a narrow temperature range, but is extrapolated for a wider temperature range, causing errors. As an example,

the extrapolated welding time for a temperature of 170°C was 0.01 seconds, which is obviously not correct. For the shorter part, the time spent at higher temperatures was greater, resulting in over estimation of the degree of healing.

4.3 Model Comparison

Under the conditions selected for the processing of ABS P400, sintering has a significant effect on bond formation, but only for the short duration of time that the temperature is higher than 200° C. Experimental observations showed that the filament temperature is below this temperature and above the glass transition point for a considerably longer period of time where the bonding is driven by the molecular diffusion at the interface. Therefore, the sintering model can be applied to the initial period when the filament temperature is above 200° C and the diffusion model is more appropriate for predicting subsequent bond strength development.

5. Conclusions

In this paper, on-line measurements of the cooling temperature profiles of extruded filaments in the FDM process were carried out. It was found that most theoretical models for the cooling profile of the extruded filaments fail to predict the temperature history of filaments embedded in a multi-layered part. Experimental measurements of the temperature profiles for different specimens and their effects on the mesostructures and mechanical properties were discussed. Based on the heat transfer analysis and the sintering experimental data, the prediction of the growth of the neck formed between adjacent filaments was evaluated using the sintering model. A non-isothermal diffusion model was used for the prediction of the bonding evolution at the interface between filaments due to molecular diffusion.

The future research will be focusing on obtaining accurate estimates for the non-isothermal diffusion model and generating predictions of bond strength development between filaments in FDM parts. Parametric studies will be conducted to investigate the effects of various process conditions on temperature histories and on the evolution of mechanical properties with time.

6. Acknowledgements

The financial support for this work was provided by the Natural Sciences and Engineering Research Council of Canada (NSERC) through Research Grants awarded to Drs. Bellehumeur and Gu.

7. References

1. Li, L., Sun, Q., Bellehumeur, C. and Gu, P., *Solid Freeform Fabrication Symposium*, Austin, TX, Aug., pp1-8 (2001).
2. Li, L., Sun, Q., Bellehumeur, C. and Gu, P., *J. Manuf. Process.* (in press, 2003).
3. M.K. Agarwala, A. Bandyopadhyay, R. van Weeren, N.A. Langrana, A. Safari, and S. C. Danforth, *Solid Freeform Fabrication Symposium*, Austin, TX (1996).
4. R. W. Gray, D. G. Baird and J. H. Bohn, *Rapid Prototyping Journal*, 4, 14-25 (1998).
5. M. Atif Yardimci, S.I. Guceri, S.C. Danforth, and M. Agarwala, *Proceedings of the Solid Freeform Fabrication Symposium*, Austin, TX, 539-548 (1996).
6. J.W. Comb, W.R. Priedeman and P.W. Turley, *Manufacturing Science and Engineering*, 68-2, 547-556 (1994).
7. P. Kulkarni and D. Dutta, *ASME Transactions: Journal of Manufacturing Science and Engineering*,

- 121, 93-103 (1999).
8. J.F.R. Matas, "Modeling the mechanical behavior of fused deposition acrylonitrile-butadiene styrene polymer components", Ph. D Dissertation, Department of Aerospace and Mechanical Engineering, Notre Dame, Indiana (1999).
 9. M. A. Yardimci and S.I. Guceri, *Proceedings of the ASME Materials Division, ASME 1995*, MD-Vol. 69-2, pp1225-1235, IMECE (1995).
 10. Thomas, J.P., Rodríguez, J.F., Modeling the fracture strength between fused deposition extruded roads, Solid Freeform Fabrication Symposium Proceeding, Austin, TX (2000)
 11. L. Li, Q. Sun, C. Bellehumeur and P. Gu, *Solid Freeform Fabrication Symposium*, Austin, TX, Aug., pp. 1-8 (2002).
 12. L. Li, P. Gu, Q. Sun and C. Bellehumeur, *Trans. NAMRI/SME*, Volume XXXI, pp. 613-620 (2003).
 13. P. R. Hornsby P. R. and A. S. Maxwell, *J.Mater. Sci.*, 27, pp. 2525-2534 (1992).
 14. S. Mazur S., and D. J. Plazek, *Prog. Org. Coat.*, 24, pp. 225-236 (1994).
 15. C. T. Bellehumeur C. T., M. Bisaria and J. Vlachopoulos, *Polym. Eng. Sci.*, Vol 37, No. 3, pp. 270-278 (1997).
 16. C. T. Bellehumeur C. T., M. Kontopoulou, and J. Vlachopoulos, *Rheol. Acta*, Vol. 37, pp. 270-278 (1998).
 17. Pokluda, C. T. Bellehumeur, and J. Vlachopoulos, *AIChE J.*, Vol. 43, pp. 3253-3256 (1997).
 18. F. Yang, R. Pitchumani, Vol.35, *Macromolecules*, pp. 3213-3224 (2002).